

# 1 Quantum Phase Transitions of Quasi-One-Dimensional Heisenberg Antiferromagnets

Munehisa Matsumoto<sup>1</sup>, Syngae Todo<sup>2</sup>, Chitoshi Yasuda<sup>3</sup>, and Hajime Takayama<sup>1</sup>

<sup>1</sup> Institute for Solid State Physics, University of Tokyo, Chiba 277-8581, Japan

<sup>2</sup> Department of Applied Physics, University of Tokyo, Tokyo 113-8656, Japan

<sup>3</sup> Computational Materials Science Center, National Institute for Materials Science, Tsukuba 305-0047, Japan

We study the ground-state phase transitions of quasi-one-dimensional quantum Heisenberg antiferromagnets by the quantum Monte Carlo method with the continuous-time loop algorithm and finite-size scaling. For a model which consists of  $S = 1$  chains with bond alternation coupled on a square lattice, we determine the ground state phase diagram and the universality class of the quantum phase transitions.

## 1.1 Why Quasi-One-Dimensional Systems?

Low-dimensional quantum antiferromagnets have attracted much attention in recent years. Due to quantum fluctuations, they often have non-trivial ground states. We investigate the ground state of quasi-one-dimensional (Q1D) Heisenberg antiferromagnets (HAF's) which consist of coupled one-dimensional (1D) spin chains with bond alternation on a square lattice. An isolated 1D uniform spin chain has no long-range order and a striking phenomenon associated with the Haldane gap [1] is known, namely, chains with integer spins have a finite excitation gap over their ground states, whereas those with half-odd-integer spins do not. On the other hand, HAF's on a spatially isotropic square lattice have the long-range Neel order in the ground state [2]. What kind of ground states do the models have that lie in the intermediate region between genuine 1D systems and two-dimensional (2D) systems? This is our question.

The ground state of a 1D bond-alternated HAF's with spin magnitude  $S = 1$  has been investigated extensively [3]. There are two gapped ground states, the Haldane phase and the dimer phase, between which a quantum phase transition of the Gaussian universality class occurs. We study the ground state of coupled  $S = 1$  bond-alternated spin chains on a square lattice. There are two ways of coupling such chains, whether we place the stronger bonds on parallel positions between the neighboring chains or place them in a zig-zag way. The arrangements of bonds are shown in Fig. 1.1. Hereafter we will refer

to the former lattice as the square lattice with columnar dimerization and the latter as that with the staggered dimerization. The Hamiltonian for the model with columnar dimerization is written as follows.

$$H = J \sum_{i,j} (S_{2i-1,j} \cdot S_{i,j} + S_{2i,j} \cdot S_{i+1,j}) + J^0 \sum_{i,j} S_{i,j} \cdot S_{i,j+1} \quad (1.1)$$

The spin operator  $S_{i,j}$  has magnitude  $S_j = 1$  and  $i,j$  denote the points on a square lattice. We consider only the nearest neighbor coupling. We set the stronger intrachain coupling unity and the antiferromagnetic interchain coupling  $J^0$  positive. The strength of bond alternation is parameterized by  $\alpha$  ( $0 < \alpha < 1$ ). The Hamiltonian of the model with staggered dimerization is similarly defined. We set the  $x$  axis parallel to the chains.

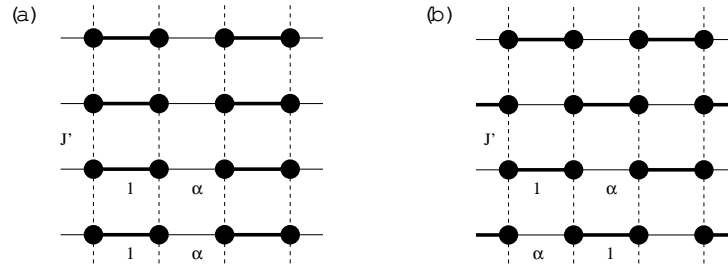


Fig. 1.1. Coupled dimerized chains on a square lattice with (a) columnar dimerization and (b) staggered dimerization

There are some previous works on coupled uniform chains [4,6] and weakly coupled bond-alternated chains on a square lattice with columnar dimerization [6]. It is known that the models have gapped ground states if the interchain coupling is weak enough and quantum phase transitions occur by tuning the interchain coupling. In our study, by using the continuous-time quantum Monte Carlo loop algorithm with the subspin-symmetrization technique [7], we determine the phase boundaries accurately and discuss the universality class of the quantum phase transition. As our method is numerically exact and non-perturbative, we can derive the ground-state phase diagram parameterized by  $\alpha$  and  $J^0$  over the whole region.

## 1.2 Simulations and Finite-Size Scaling

### 1.2.1 Details of Simulations

Let us denote the size of the lattice simulated by  $L_x, L_y$  and the temperature  $T = 1/\beta$ . By the Suzuki-Trotter decomposition, we map the original quantum

system on  $L_x \times L_y$  lattice to a classical system on  $L_x \times L_y$  spacetime by adding the imaginary-time axis (denoted by  $\tau$ ) with the length  $\beta$ . The aspect ratios  $L_x=L_y$ ,  $L_x=2$ , are fixed. Fixing the ratios between the spatial size and the imaginary-time size is based on the assumption of Lorentz invariance [8], namely, the dynamical critical exponent be equal to unity. The sizes of the simulated systems and inverse temperatures are up to  $L_x \times L_y = 10^3$  sites and  $\beta = 10^2$ , with  $10^3$  Monte Carlo steps used for thermalization and  $10^4$  for measurement. The latter are cut into 20 bins from which we obtain averages and variances as estimates of observables and their statistical errors.

We calculate the staggered susceptibility  $\chi_s$ , correlation lengths  $\xi_x, \xi_y$  and the excitation gap  $\Delta$ . Correlation lengths are calculated from the second moment of correlation functions and the gap is obtained as a reciprocal number of  $\Delta$ . By the finite-size scaling (FSS) of these observables, we determine critical points and exponents in the thermodynamic limit  $L_x, L_y \rightarrow \infty$  and the ground state limit  $\beta \rightarrow \infty$ . We obtain critical exponents of the staggered susceptibility  $\chi_s$  and the correlation length  $\xi$ , by which the critical behavior of  $\chi_s$  and  $\xi$  are described as  $\chi_s \sim t^{-\nu}$  and  $\xi \sim t^{-\nu}$ , where  $t$  is the distance from the critical point. These are sufficient to give other exponents with the scaling relations.

### 1.2.2 Determination of critical points and exponents

We fit the behavior of observables near critical points into the FSS formulae which are written as  $\chi_s = L f_d(tL^{1/\nu})$  and  $\xi = L^{-1} g(tL^{1/\nu})$ , where  $L$  is the linear system size and  $f_d, g$  are polynomials. We take terms of the polynomial up to the second order. Here we describe how the critical point and exponents are determined in the ground state of staggeredly coupled bond alternating chains with  $\delta = 0.1$ . The raw data of the staggered susceptibility  $\chi_s$  are plotted in Fig. 1.2 (a) and its FSS is shown in Fig. 1.2 (b). Data with  $L_x = L_y = 16, 24$ , and  $32$  are used. As seen in Fig. 1.2, the data near the critical point are scaled quite well by choosing  $J_c^0$ ,  $\nu$  and  $\Delta$  as  $0.1943(4)$ ,  $0.69(2)$  and  $1.4(1)$ , respectively. These exponents coincide with those of 3D classical Heisenberg models  $\nu = 0.7048(30)$  and  $\Delta = 1.3873(85)$  [9] within numerical accuracy. It is thus confirmed that the universality class of the quantum phase transition of the 2D quantum Heisenberg model belongs to that of 3D classical Heisenberg models. The FSS on correlation lengths gives consistent results.

Other critical points are determined in the same way to yield the phase boundary over the whole parameter region.

## 1.3 Results and Discussions

In Fig. 1.3, we present the ground-state phase diagrams for columnar and staggered dimerization. First of all, both of them are quite similar with each

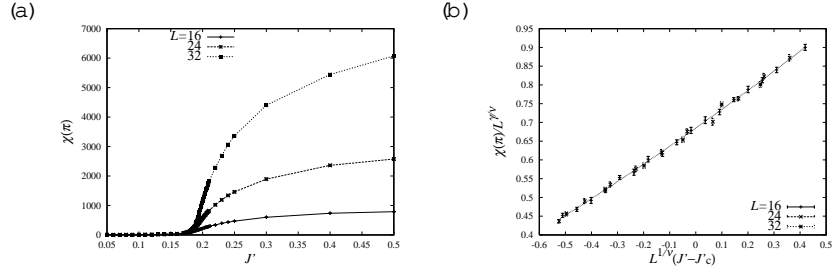


Fig. 1.2. (a) Raw data plot of the staggered susceptibility and (b) its finite-size scaling plot, with  $L$  denoting the system size simulated

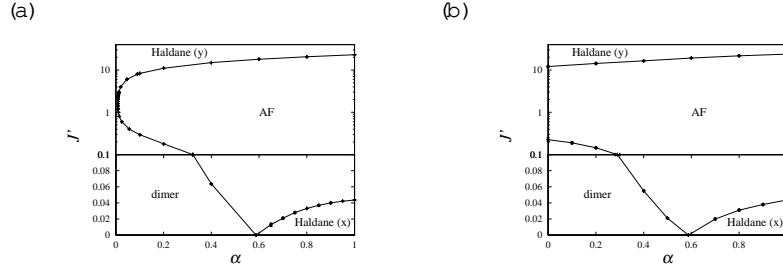


Fig. 1.3. Ground-state phase diagrams of the model on a square lattice with (a) columnar dimerization and (b) staggered dimerization

other for large  $J^0$ . Actually these two models are identical on the line with  $\alpha = 1.0$ . On this line, there are three points which have been investigated in detail so far. The 2D isotropic HAF at  $(\alpha; J^0) = (1; 1)$  has a gapless ground state with finite staggered magnetization. The AF phase, which includes the isotropic point, occupies a large area in the phase diagram. On the other hand, the system consists of decoupled Haldane chains parallel to the  $x$  ( $y$ ) axis in the  $J^0 = 0$  ( $J^0 \rightarrow 1$ ) limit. The finite excitation gap (Haldane gap) observed at  $J^0 = 0$  and 1 survives even at finite  $J^0$ . We refer to these two gapped phases as Haldane (x) and Haldane (y) phases, respectively.

Now we take a more detailed look on the models with columnar dimerization. At  $(\alpha; J^0) = (0; 0)$ , the system consists of decoupled dimers and therefore has a spin-gapped ground state (dimer phase). This phase also extends to finite  $\alpha$  and  $J^0$ . Most striking feature of the phase diagram shown in Fig. 1.3 (a) is that the dimer phase around  $(\alpha; J^0) = (0; 0)$  and the Haldane (y) phase at large  $J^0$  are actually the identical phase. Since the boundary of the AF phase does not touch the  $\alpha = 0$  line, there is no critical point between the dimer and Haldane (y) phases. Especially it should be pointed out that the  $\alpha = 0$  line corresponds to the two-leg ladders, which always has a spin-gapped ground state irrespective of the strength of rung coupling [10].

Furthermore, the Haldane (x) and Haldane (y) phases are also shown to be identical by considering the bond alternation in the  $y$  direction [11]. Thus

in the ground states of Q1D models, all of the gapped phases are identical. On the other hand, in a strictly 1D chain, the dimer phase and the Haldane phase are definitively distinguished in terms of the topological hidden order measured by the string-order parameter [12], which is non-zero only in the Haldane phase. It should be emphasized that once we have a finite interchain coupling the string-order parameter vanishes even in the Haldane (x) phase. In this sense the line  $J^0 = 0$ , which represents strictly 1D chains, is singular in the phase diagram.

The ground-state phase diagram of the model with staggered dimerization is topologically different from the columnar one. Particularly the AF phase extends onto the  $J^0 = 0$  line, as the lattice remains connected two-dimensionally even at  $J^0 = 0$  (as long as  $J^0$  is finite). Thus in the phase diagram three spin-gapped phases (Haldane (x), Haldane (y) and dimer) are separated by the AF phase. It is of great interest to pursue phase diagrams in the presence of the bond alternation in the y direction both in columnar and staggered ways and see the topology of these gapped phases in the extended parameter space.

## References

1. F. D. M. Haldane: Phys. Lett. A 93, 464 (1983); Phys. Rev. Lett. 50, (1983) 1153 (1983)
2. K. Kubo and T. Kishi: Phys. Rev. Lett. 61, 2585 (1988)
3. I. A. A. Eck and F. D. M. Haldane: Phys. Rev. B 36, 5291 (1987); R. R. P. Singh and M. P. Gelfand: Phys. Rev. Lett. 61, 2133 (1988); Y. Kato and A. Tanaka: J. Phys. Soc. Jpn. 63, 1277 (1994); S. Yamamoto: Phys. Rev. B 51, 16128 (1995); 52, 10170 (1995); A. Kitazawa, K. Nomura, and K. Okamoto: Phys. Rev. Lett. 76, 4038 (1996); A. Kitazawa and K. Nomura: J. Phys. Soc. Jpn. 66, 3379 (1997); 66, 3944 (1997); M. Kohno, M. Takahashi, and M. Hagiwara: Phys. Rev. B 57, 1046 (1998); M. Nakamura and S. Todo: Phys. Rev. Lett. 89, 077204 (2002)
4. T. Sakai and M. Takahashi: J. Phys. Soc. Jpn. 58, 3131 (1989)
5. H. Tasaki: Phys. Rev. Lett. 64, 2066 (1990)
6. A. Koga and N. Kawakami: Phys. Rev. B 61, 6133 (2000)
7. S. Todo and K. Kato: Phys. Rev. Lett. 87, 047203 (2001); B. B. Beard and U.-J. Wiese: Phys. Rev. Lett. 77, 5130 (1996); H. G. Evertz: Adv. Phys. 52, 1 (2003)
8. S. Chakravarty, B. I. Halperin, and D. R. Nelson: Phys. Rev. Lett. 60, 1057 (1988); Phys. Rev. B 39, 2344 (1989)
9. K. Chen, A. M. Ferrenberg, and D. P. Landau: Phys. Rev. B 48, 3249 (1993)
10. S. Todo, M. Matsumoto, C. Yasuda, and H. Takayama: Phys. Rev. B 64, 224412 (2001)
11. M. Matsumoto, C. Yasuda, S. Todo, and H. Takayama: Phys. Rev. B 65, 014407 (2002)
12. M. den Nijs and K. Rommelse: Phys. Rev. B 40, 4709 (1989); H. Tasaki: Phys. Rev. Lett. 66, 798 (1991)